Available online at www.sciencedirect.com
SCIENCE DIRECT®
Journal of Organometallic Chemistry 689 (2004) 3218–3231
Journal of Organometallic Chemistry
www.elsevier.com/locate/jorganchem

Synthesis, structures and comparative electrochemical study of 2,5-bis(trimethylsilylethynyl)thiophene coordinated cobalt carbonyl units

Avelina Arnanz [a], Maria-Luisa Marcos [b,*], Consuelo Moreno [a], David H. Farrar [c], Allan J. Lough [c], Joanne O. Yu [c], Salomé Delgado [a], Jaime González-Velasco [b]

[a] *Departamento de Química Inorgánica de la Universidad Autónoma de Madrid, 28049 Madrid, Spain*
[b] *Departamento de Química de la Universidad Autónoma de Madrid, Spain*
[c] *Lash Miller Chemical Laboratories, University of Toronto, 80 St. George Street, Toronto, Canada M5S 3H6*

Received 10 June 2004; accepted 20 July 2004
Available online 19 August 2004

Abstract

The reaction between 2,5-bis(trimethylsilylethynyl)thiophene and $Co_2(CO)_8$ or $Co_2(CO)_6(X)$, (X = dppa, dppm), gave rise to the formation of substituted ethynylcobalt complexes containing one or two $Co_2(CO)_6$ or $Co_2(CO)_4(X)$ units, 2-[$Co_2(CO)_4(X)\{\mu_2$-η^2-$(SiMe_3)C_2\}$]-5-$(Me_3SiC{\equiv}C)C_4H_2S$ (X = 2CO (**1**), dppa (**3**) or dppm (**4**)) and 2,5-[$Co_2(CO)_4(X)\{\mu_2$-η^2-$SiMe_3C_2\}]_2C_4H_2S$ (X = 2CO (**2**), dppa (**5**) or dppm (**6**)). Desilylation of the non-metallated and metallated alkynes in **3**, **4** and **6** occurred on treatment with KOH and tetrabutylammonium fluoride to give 2-[$Co_2(CO)_4(\mu$-X)$\{\mu_2$-η^2-$SiMe_3C_2\}$]-5-$(C{\equiv}CH)C_4H_2S$ (X = dppa (**7**), dppm (**8**)) and 2,5-[$Co_2(CO)_4(\mu$-dppm)$\{\mu_2$-η^2-$HC_2\}]_2C_4H_2S$ (**9**), respectively. Crystals of **6** suitable for single-crystal X-ray diffraction were grown and the molecular structure of this compound is discussed. A comparative electrochemical study of all these complexes is presented by means of the cyclic and square-wave voltammetry techniques.

Keywords: Thiophene; Cobalt carbonyl complexes; Electrochemistry

1. Introduction

The chemistry of alkynes coordinated to transition metals has been extensively studied and is well established [1]. The interest in this kind of complexes is due, in part, to the stabilising influence of the metal on reactive unsaturated carbon chains and polycarbon ligands [1,2] and, on the other hand, to their potential optoelectronic properties as non-linear optical and electroluminescent materials [3], or as "molecular" wires [4,5]. Thus alkynyl or polyynediyl bridging ligands have been shown to be especially efficient in allowing the passage of electronic effects between redox active centres [6–8] and therefore the electronic properties can be modified by changing both, metal fragments and/or alkyne ligands [9]. The electronic communication through such potential molecular wires is often evaluated by studying the redox response of electroactive groups [10].

In recent studies we have observed that complexes where the redox centres are either $Co_2(CO)_6$ or $Co_2(CO)_4$dppm linked by 1,3,5-tris(trimethylsilylethynyl)benzene [7] and 1,4-bis(trimethylsilyl)butadiyne [8] ligands show electronic communication between the metal centres. In order to study the ability of the metals to participate in π delocalisation we have now investigated the electronic communication between $Co_2(CO_6)$, $Co_2(CO)_4$dppm and $Co_2(CO)_4$dppa moieties linked by

* Corresponding author. Tel.: +3491 49 78665; fax: +3491 49 75238.
E-mail address: mluisa.marcos@uam.es (M.-L. Marcos).

0022-328X/$ - see front matter © 2004 Elsevier B.V. All rights reserved.
doi:10.1016/j.jorganchem.2004.07.028

2,5-bis(trimethylsilylethynyl)thiophene. We report here the synthesis, characterization and the redox properties of these compounds.

2. Experimental

2.1. Reagents and general techniques

All manipulations were carried out by using standard Schlenk vacuum-line and syringe techniques under an atmosphere of oxygen-free Ar. All solvents for synthetic use were reagent grade. Diethyl ether, hexane and tetrahydrofurane (THF) were dried and distilled over sodium in the presence of benzophenone under an Ar atmosphere. Also under Ar, CH_2Cl_2 was dried and distilled over CaH_2. Methanol was stored over molecular sieves (4 Å) under Ar. All solvents were bubbled with Ar for 1 h after distillation and then stored under Ar or degassed by means of at least three freeze–pump–thaw cycles after distillation and before use. Column chromatography was performed by using silica gel 100 (Fluka) and preparative TLC on 20×20 cm glass plates coated with silica gel (SDS 60–17 μm, 0.25 mm thick). $Me_3SiC{\equiv}CH$ (TMSA), 2,5-dibromothiophene, $Co_2(CO)_8$, KOH (Fluka), 1,2-bis(diphenylphosphino)methane (dppm), CuI and a solution 1.0 M of tetrabutylammonium fluoride (TBAF) in THF (Aldrich) were used as received. Trimethylamine *N*-oxide (Aldrich) was sublimed prior to use and stored under Ar. The compounds 1,2-bis(diphenylphosphino)amine (dppa) [11], $Co_2(CO)_6$(dppm) [12], $Co_2(CO)_6$(dppa) [13,14], $Pd(PPh_3)_4$[15] and 2,5-bis(trimethylsilylethynyl)thiophene [16] were prepared according to the literature and characterized by their IR and NMR spectra. The ^1H, ^{13}C, ^{31}P, proton-decoupled ^{31}P NMR spectra and HMQC (heteronuclear multiple quantum correlation) and HMBC (heteronuclear multiple bond correlation) experiments were recorded on a Bruker AMX-300 and 500 instrument. Chemical shifts were measured relative either to an internal reference of tetramethylsilane or to residual protons of the solvents. The coupling constant errors are ±0.5 Hz. Infrared spectra were measured on a Perkin–Elmer 1650 infrared spectrometer. Elemental analyses were performed by the Mycroanalytical Laboratory of the University Autónoma of Madrid on a Perkin–Elmer 240 B microanalyser. Electronic spectra were recorded on a Unicam UV 4 UV–Vis spectrophotometer. Mass spectra were measured on a VG-Autospec mass spectrometer for FAB by the Mass Laboratory of the University Autónoma of Madrid. Electrochemical measurements were carried out with a computer driven Par Mo. 273 electrochemistry system in a three electrode cell under N_2 atmosphere in anhydrous deoxygenated solvents (CH_2Cl_2 and THF) containing 0.2 M tetrabutylammonium hexafluorophosphate ($TBAPF_6$) as supporting electrolyte. Cyclic and square-wave voltammetry (CV and SWV, respectively) studies were made in a three-electrode system. Polycrystalline Pt (0.05 cm^2) or glassy carbon were used as working electrodes; the counter electrode was a Pt gauze and the reference electrode was a silver wire quasi-reference electrode. Decamethylferrocene (Fc*) was used as internal standard, and all potentials in this work are referred to the Fc^{*+}/Fc* couple. Under the actual experimental conditions, $E_{1/2}$ of the ferrocene couple (Fc^+/Fc) was +0.44 V vs. Fc^{*+}/Fc* in THF solution and +0.55 V vs. Fc^{*+}/Fc* in CH_2Cl_2 solution.

2.2. Synthesis of 2-[$Co_2(CO)_6\{\mu_2$-η^2-$SiMe_3C_2\}$]-5-($Me_3SiC{\equiv}C$)C_4H_2S (**1**) and 2,5-[$Co_2(CO)_6\{\mu_2$-η^2-$SiMe_3C_2\}]_2C_4H_2S$ (**2**)

To a solution of 2,5-bis(trimethylsilylethynyl)thiophene (0.60 g, 2.16 mmol) in hexane (100 mL) was added 1.5 equiv. of $Co_2(CO)_8$. The reaction was monitored by FT-IR and ^1H NMR. After the mixture was stirred for 1 h at room temperature, the solvent was removed under vacuum and the residue was eluted with hexane on a silica column to afford **1** (52% yield) and **2** (42% yield) as an unstable dark red and green solid, respectively. **2** has also been obtained as an only product in high yield (97%) from 2,5-bis(trimethylsilylethynyl)thiophene (0.30 g, 1.08 mmol) and 2 equiv. of $Co_2(CO)_8$ and subsequent chromatography with hexane on a silica column.

(**1**) IR (hexane, cm^{-1}): $\nu_{C{\equiv}C}$ 2151.1 (vw); ν_{CO} 2088.2 (m), 2054.6 (s), 2028.0 (vs). ^1H NMR (300 MHz, $CDCl_3$, ppm): δ 7.11 (d, H_4, J_{HH} = 3.9 Hz); 7.09 (d, H_5, J_{HH} = 3.9 Hz); 0.39 (s, 9H, –$CSiMe_3$); 0.24 (s, 9H, ≡$CSiMe_3$). ^1H NMR (300 MHz, CD_2Cl_2, ppm): δ 7.13 (d, H_4, J_{HH} = 3.8 Hz); 7.11 (d, H_5, J_{HH} = 3.8 Hz); 0.40 (s, 9H, –$CSiMe_3$); 0.24 (s, 9H, ≡$CSiMe_3$). ^{13}C NMR (125 MHz, $CDCl_3$, ppm): δ 199.3 (m, CO); 143.5 (s, C_3); 133.7 (s, C_5); 128.8 (s, C_4); 123.6 (s, C_6); 100.5 (s, C_8); 97.2 (s, C_7); 93.3 (s br, C_2); 81.1 (s br, C_1); 0.62 (s, –$CSiMe_3$); −0.28 (s, ≡$CSiMe_3$). UV–V (CH_2Cl_2, nm): λ_{max} 568, 446 (sh) and 230. MS (FAB^+, *m*/*z*): 534.0 [M^+ − CO].

(**2**) IR (hexane, cm^{-1}): ν_{CO} 2086.0 (m), 2055.0 (s), 2027.8 (vs). ^1H NMR (300 MHz, $CDCl_3$, ppm): δ 7.15 (s, $H_{4,4'}$); 0.40 (s, 18H, 2 –$SiMe_3$). ^{13}C NMR (125 MHz, $CDCl_3$, ppm): δ 199.8 (m, CO); 142.8 (s, $C_{3,3'}$); 130.7 (s, $C_{4,4'}$); 94.1 (s br, $C_{2,2'}$); 81.5 (s br, $C_{1,1'}$); 1.04 (s, 2 –$SiMe_3$). UV–Vis (CH_2Cl_2, nm): λ_{max} 595, 450 (sh) and 229. MS (FAB^+, *m*/*z*): 820.0 [M^+ − CO].

2.3. Synthesis of 2-[$Co_2(CO)_4(\mu$-X)$\{\mu_2$-η^2-$SiMe_3C_2\}$]-5-($Me_3SiC{\equiv}C$)C_4H_2S. X = dppa (**3**) and X = dppm (**4**)

2.3.1. Method A

A solution of **1** (0.50 g, 0.89 mmol) and 0.89 mmol of dppa or dppm in hexane (100 mL) was prepared.

Trimethylamine *N*-oxide (0.20 g, 1.78 mmol) was added and the reaction mixture, monitored by FT-IR, was stirred at 40 °C for 3 days. After the solvent was removed under vacuum, the product was purified by thin-layer chromatography (TLC) using hexane/CH_2Cl_2 (3:1) or by hexane-packed silica column (200 g) using the same eluent to afford the stable red solids **3** (65% yield) or **4** (70% yield), respectively.

2.3.2. Method B

A suspension of $Co_2(CO)_6$(dppa) or $Co_2(CO)_6$(dppm) (1.95 mmol) in hexane (50 mL) was added to a solution of 2,5-bis(trimethylsilylethynyl)thiophene (0.54 g, 1.95 mmol) in the same solvent. The reaction mixture was stirred at 65 °C for 15 days. Complex **3** or **4** were isolated in 28% and 33% yields, respectively, in the same manner used in *Method A*.

(**3**) IR (CH_2Cl_2, cm^{-1}): ν_{NH} 3321.8 (w); $\nu_{C\equiv C}$ 2137.2 (w); ν_{CO} 2025.5 (s), 1997.9 (vs), 1971.5 (s), 1957.4 (sh). ^1H NMR (300 MHz, $CDCl_3$, ppm): δ 7.42–7.28 (m, 20H, Ph); 6.60 (d, H_5, J_{HH} = 3.8 Hz); 5.87 (d, H_4, J_{HH} = 3.8 Hz); 3.95 (t, –NH, J_{PH} = 6.4 Hz); 0.37 (s, 9H, –$CSiMe_3$); 0.24 (s, 9H, ≡$CSiMe_3$). ^{13}C NMR (125 MHz, $CDCl_3$, ppm): δ 206.3 (m, CO); 203.2 (m, CO); 148.5 (t, J_{CP} = 4.3 Hz, C_3); 142.0 (t, J_{CP} = 22.2 Hz, *i*-Ph); 139.0 (t, J_{CP} = 23.2 Hz, *i*-Ph); 133.2 (s, C_5); 131.0 (t, J_{CP} = 6.8 Hz, *o*-Ph); 130.6 (t, J_{CP} = 6.7 Hz, *o*-Ph); 130.3 (s, *p*-Ph); 130.1 (s, *p*-Ph); 128.8 (t, J_{CP} = 4.9 Hz, *m*-Ph); 128.7 (t, J_{CP} = 4.9 Hz, *m*-Ph); 128.5 (s, C_4); 120.7 (s, C_6); 98.9 (s) and 98.6 (s), (C≡C); 92.1 (m, C_2); 91.1 (m, C_1); 1.42 (s, –$CSiMe_3$); 0.37 (s, ≡$CSiMe_3$). ^{31}P NMR (121 MHz, $CDCl_3$, ppm): δ 91.7 (s br, 2P, dppa). UV–Vis (CH_2Cl_2, nm): λ_{max} 552 and 229. MS (FAB^+, *m/z*): 863.0 [M^+ – CO]; 807.0 [M^+ – 3CO]; 779.0 [M^+ – 4CO]. Anal. Calc. for $C_{42}H_{41}O_4Co_2SP_2Si_2N$: C, 56.67; H, 4.59; N, 1.59. Found: C, 56.52; H, 4.63; N, 1.53%.

(**4**) IR (CH_2Cl_2, cm^{-1}): $\nu_{C\equiv C}$ 2137.7 (w); ν_{CO} 2021.3 (s), 1995.2 (vs), 1967.9 (s), 1948.7 (sh). ^1H NMR (300 MHz, $CDCl_3$, ppm): 7.32–6.98 (m, 20H, Ph); 6.96 (d, H_5, J_{HH} = 3.7 Hz); 6.46 (d, H_4, J_{HH} = 3.7 Hz); 3.60 (dt, J_{HH} = 13.1 Hz, J_{PH} = 10.5 Hz, 1H, ABXY, –CH_2–); 3.37 (dt, J_{HH} = 13.2 Hz, J_{PH} = 10.3 Hz, 1H, ABXY, –CH_2–); 0.36 (s, 9H, –$CSiMe_3$); 0.26 (s, 9H, ≡$CSiMe_3$). ^{13}C NMR (125 MHz, $CDCl_3$, ppm): δ 206.9 (m, CO); 202.2 (m, CO); 150.7 (t, J_{CP} = 3.8 Hz, C_3); 138.5 (t, J_{CP} = 24.1 Hz, *i*-Ph); 134.6 (t, J_{CP} = 17.2 Hz, *i*-Ph); 133.2 (s, C_5); 132.6 (t, J_{CP} = 6.3 Hz, *o*-Ph); 130.6 (t, J_{CP} = 5.9 Hz, *o*-Ph); 129.8 (s, *p*-Ph); 129.3 (s, *p*-Ph); 128.5 (t, J_{CP} = 4.6 Hz, *m*-Ph); 128.0 (t, J_{CP} = 4.7 Hz, *m*-Ph); 126.0 (s, C_4); 121.0 (s, C_6); 98.7 (s) and 98.2 (s), (C≡C); 93.1 (m, C_2); 89.9 (m, C_1); 36.5 (t, J_{CP} = 20.3 Hz, –CH_2–); 0.82 (s, –$CSiMe_3$); 0.00 (s, ≡$CSiMe_3$). ^{31}P NMR (121 MHz, $CDCl_3$, ppm): δ 35.0 (s br, 2P, dppm). UV-V (CH_2Cl_2, nm): λ_{max} 544 and 230. MS (FAB^+, *m/z*): 891.0 [M^+]; 863.0 [M^+ – CO]; 835.0 [M^+ – 2CO]; 807.0 [M^+ – 3CO]; 779.0 [M^+ – 4CO]. Anal. Calc. for $C_{43}H_{42}O_4Co_2SP_2Si_2$: C, 58.22; H, 4.72. Found: C, 57.97; H, 4.74%.

2.4. Synthesis of 2,5-[$Co_2(CO)_4(\mu$-X)$\{\mu_2$-η^2-Si$Me_3C_2\}]_2C_4H_2S$. X = dppa (**5**) and X = dppm (**6**)

The same procedure as described above was followed in the preparation of these compounds. For the *Method A* from **2** (0.40 g, 0.47 mmol), dppa or dppm (0.94 mmol) and trimethylamine *N*-oxide (0.21 g, 1.88 mmol). For the *Method B* from 2,5-bis(trimethylsilylethynyl)thiophene (0.20 g, 0.72 mmol) and the derivative $Co_2(CO)_6$(dppa) or $Co_2(CO)_6$(dppm) (1.44 mmol). After the solvent was removed under vacuum, the product was purified by thin-layer chromatography (TLC) using hexane/CH_2Cl_2 (3:1) or by hexane-packed silica column (200 g) using the same eluent to afford the stable green solids **5** (60% and 25% yields for the *Methods A* and *B*, respectively) or **6** (65% and 30% yields for the *Methods A* and *B*, respectively).

(**5**) IR (CH_2Cl_2, cm^{-1}): ν_{NH} 3321.8 (w); ν_{CO} 2020.8 (s), 1994.0 (vs), 1966.7 (s), 1952.6 (sh). ^1H NMR (300 MHz, $CDCl_3$, ppm): δ 7.42–7.14 (m, 40H, Ph); 5.26 (s, $H_{4,4'}$); 3.95 (t, 2 –NH, J_{PH} = 6.5 Hz); 0.37 (s, 18H, 2 –$SiMe_3$). ^{13}C NMR (125 MHz, $CDCl_3$, ppm): δ 206.2 (m, CO); 203.6 (m, CO); 142.8 (m, $C_{3,3'}$); 142.4 (t, J_{CP} = 22.1 Hz, *i*-Ph); 139.1 (t, J_{CP} = 22.1 Hz, *i*-Ph); 131.2 (t, J_{CP} = 6.8 Hz, *o*-Ph); 130.6 (t, J_{CP} = 6.8 Hz, *o*-Ph); 130.1 (s, *p*-Ph); 129.9 (s, *p*-Ph); 128.8 (t, J_{CP} = 4.7 Hz, *m*-Ph); 128.7 (s, $C_{4,4'}$); 128.5 (t, J_{CP} = 4.8 Hz, *m*-Ph); 92.4 (m, $C_{2,2'}$); 89.0 (m, $C_{1,1'}$); 1.43 (s, 2 –$SiMe_3$). ^{31}P NMR (121 MHz, $CDCl_3$, ppm): δ 92.0 (s br, 4P, 2 dppa). UV–Vis (CH_2Cl_2, nm): λ_{max} 591, 404 and 230. MS (FAB^+, *m/z*): 1478.0 [M^+ – CO]; 1450.1 [M^+ – 2CO]; 1310.2 [M^+ – 7CO]; 1282.2 [M^+ – 8CO]. Anal. Calc. for $C_{70}H_{62}O_8Co_4SP_4Si_2N_2$: C, 55.69; H, 4.11; N, 1.86. Found: C, 55.82; H, 4.10; N, 1.83%.

(**6**) IR (CH_2Cl_2, cm^{-1}): ν_{CO} 2017.6 (s), 1994.5 (vs), 1965.0 (s), 1945.0 (sh). ^1H NMR (300 MHz, $CDCl_3$, ppm): δ 7.24–6.97 (m, 40H, Ph); 6.56 (s, $H_{4,4'}$); 3.60 (dt, J_{HH} = 13.1 Hz, J_{PH} = 10.5 Hz, 2H, ABXY, 2 –CH_2–); 3.47 (dt, J_{HH} = 13.2 Hz, J_{PH} = 10.3 Hz, 2H, ABXY, 2 –CH_2–); 0.40 (s, 18H, 2 –$SiMe_3$). ^{13}C NMR (125 MHz, $CDCl_3$, ppm): δ 206.8 (m, CO); 202.5 (m, CO); 145.8 (t, J_{CP} = 2.9 Hz, $C_{3,3'}$); 138.5 (t, J_{CP} = 24.1 Hz, *i*-Ph); 134.7 (t, J_{CP} = 17.1 Hz, *i*-Ph); 132.6 (t, J_{CP} = 6.3 Hz, *o*-Ph); 130.7 (t, J_{CP} = 6.1 Hz, *o*-Ph); 129.5 (s, *p*-Ph); 129.2 (s, *p*-Ph); 128.4 (t, J_{CP} = 4.6 Hz, *m*-Ph); 127.8 (t, J_{CP} = 4.6 Hz, *m*-Ph); 127.2 (s, $C_{4,4'}$); 93.5 (t, J_{CP} = 6.5 Hz, $C_{2,2'}$); 89.5 (t, J_{CP} = 9.8 Hz, $C_{1,1'}$); 37.9 (t, J_{CP} = 19.6 Hz, 2 –CH_2–); 1.09 (s, 2 –$SiMe_3$). ^{31}P NMR (121 MHz, $CDCl_3$, ppm): δ 34.8 (s br, 4P, 2 dppm). UV–Vis (CH_2Cl_2, nm): λ_{max} 577, 403 and 229. MS (FAB^+, *m/z*): 1475.9 [M^+ – CO]; 1447.8 [M^+ – 2CO]; 1419.8 [M^+ – 3CO]; 1307.9 [M^+ – 7CO];

1279.9 [$M^+ - 8CO$]. Anal. Calc. for $C_{72}H_{64}O_8Co_4SP_4Si_2$: C, 57.59; H, 4.26. Found: C, 57.45; H, 4.28%.

2.5. Synthesis of 2-[$Co_2(CO)_4(\mu$-X)$\{\mu_2$-η^2:η^2–$SiMe_3$-$C_2\}$]-5-($C{\equiv}CH$)C_4H_2S X = dppa (7) and X = dppm (8)

2.5.1. Method A

3 or **4** (0.62 mmol) was dissolved in a MeOH solution saturated with KOH and the mixture was stirred for 24 h at 25 °C. After that, the solvent was removed under vacuum and the residue was extracted with several portions of Et_2O and purified by hexane-packed silica column (200 g) using hexane/CH_2Cl_2 (1:1) as eluent to afford the unstable red solids **7** (53% yield) or **8** (58% yield).

2.5.2. Method B

To a solution of **3** or **4** (0.56 mmol) in THF/MeOH (10:1) was added TBAF (1.15 mL, 1.0 M in THF, 1.15 mmol) and the mixture was stirred for 24 h at room temperature. After the solvent was removed under vacuum, the product was purified by hexane-packed silica column using hexane/CH_2Cl_2 (1:1) as eluent to afford **7** or **8** in 18% and 21% yield, respectively.

(**7**) IR (CH_2Cl_2, cm^{-1}): ν_{NH} 3328.2 (w); $\nu_{{\equiv}CH}$ 3305.6 (m); $\nu_{C{\equiv}C}$ 2095.9 (vw); ν_{CO} 2028.7 (s), 2001.6 (vs), 1974.8 (s), 1957.7 (sh). ^{1}H NMR (300 MHz, $CDCl_3$, ppm): δ 7.46–7.28 (m, 20H, Ph); 6.64 (d, H_5, J_{HH} = 3.9 Hz); 5.92 (d, H_4, J_{HH} = 3.8 Hz); 3.94 (t, –NH, J_{PH} = 6.3 Hz); 3.32 (s, 1H, ≡CH); 0.37 (s, 9H, –$SiMe_3$). ^{13}C NMR (125 MHz, $CDCl_3$, ppm): δ 206.3 (m, CO); 203.2 (m, CO); 149.1 (t, J_{CP} = 3.8 Hz, C_3); 142.0 (t, J_{CP} = 21.1 Hz, *i*-Ph); 139.0 (t, J_{CP} = 23.0 Hz, *i*-Ph); 133.5 (s, C_5); 130.9 (t, J_{CP} = 6.8 Hz, *o*-Ph); 130.6 (t, J_{CP} = 6.8 Hz, *o*-Ph); 130.2 (s, *p*-Ph); 130.1 (s, *p*-Ph); 128.8 (t, J_{CP} = 4.8 Hz, *m*-Ph); 128.7 (t, J_{CP} = 4.8 Hz, *m*-Ph); 128.1 (s, C_4); 119.5 (s, C_6); 91.9 (t, J_{CP} = 11.0 Hz, C_2); 91.1 (m, C_1); 81.1 (s, C_8); 78.2 (s, C_7); 1.42 (s, –$SiMe_3$). ^{31}P NMR (121 MHz, $CDCl_3$, ppm): δ 91.7 (s br, 2P, dppa). UV–Vis (CH_2Cl_2, nm): λ_{max} 547 (sh) and 231. MS (FAB^+, *m/z*): 792.1 [$M^+ - CO$]; 736.1 [$M^+ - 3CO$]; 708.1 [$M^+ - 4CO$].

(**8**) IR (CH_2Cl_2, cm^1): $\nu_{C{\equiv}H}$ 3300.4 (m); $\nu_{C{\equiv}C}$ 2094.9 (vw); ν_{CO} 2021.7 (s), 1996.1 (vs), 1968.3 (s), 1952.6 (sh). ^{1}H NMR (300 MHz, $CDCl_3$, ppm): δ 7.32–6.98 (m, 20H, Ph); 7.01 (d, H_5, J_{HH} = 3.7 Hz); 6.51 (d, H_4, J_{HH} = 3.7 Hz); 3.60 (dt, J_{HH} = 13.1 Hz, J_{PH} = 10.4 Hz, 1H, ABXY, –CH_2–); 3.38 (dt, J_{HH} = 13.2 Hz, J_{PH} = 10.3 Hz, 1H, ABXY, –CH_2–); 3.37 (s, 1H, ≡CH); 0.37 (s, 9H, –$SiMe_3$). ^{13}C NMR (125 MHz, $CDCl_3$, ppm): δ 205.9 (m, CO); 201.1 (m, CO); 150.0 (t, J_{CP} = 2.9 Hz, C_3); 137.4 (t, J_{CP} = 24.1 Hz, *i*-Ph); 133.5 (t, J_{CP} = 16.9 Hz, *i*-Ph); 132.5 (s, C_5); 131.6 (t, J_{CP} = 6.0 Hz, *o*-Ph); 129.5 (t, J_{CP} = 6.0 Hz, *o*-Ph); 128.7 (s, *p*-Ph); 128.3 (s, *p*-Ph); 127.4 (t, J_{CP} = 4.6 Hz, *m*-Ph); 126.9 (t, J_{CP} = 4.6 Hz, *m*-Ph); 124.7 (s, C_4); 118.6 (s, C_6); 93.0 (m, C_2); 91.1 (m, C_1); 80.1 (s, C_8); 76.5 (s, C_7); 36.1 (m, –CH_2–); 0.00 (s, –$SiMe_3$). ^{31}P NMR (121 MHz, $CDCl_3$, ppm): δ 34.9 (s br, 2P, dppm). UV–Vis (CH_2Cl_2, nm): λ_{max} 536 (sh) and 231. MS (FAB^+, *m/z*): 791.1 [$M^+ - CO$]; 735.1 [$M^+ - 3CO$]; 707.1 [$M^+ - 4CO$].

2.6. Synthesis of 2,5-[$Co_2(CO)_4(\mu$-dppm)$\{\mu_2$-η^2-$HC_2\}]_2C_4H_2S$ (9)

The same procedure as described above in *Method B* was carried out from compound **6** (0.24 g, 0.16 mmol) and TBAF (1.33 mL, 1.0 M in THF, 1.33 mmol). After the solvent was removed under vacuum, the product was purified in the same manner to afford the unstable green solid **9** (55% yield).

(**9**) IR (CH_2Cl_2, cm^1): ν_{CO} 2022.3 (s), 1997.3 (vs), 1968.4 (s), 1951.0 (sh). ^{1}H NMR (300 MHz, $CDCl_3$, ppm): δ 7.42–7.16 (m, 40H, Ph); 7.14 (s, $H_{4,4'}$); 5.78 (t, 2 –CH, J_{PH} = 6.2 Hz); 3.56 (dt, J_{HH} = 13.1 Hz, J_{PH} = 10.6 Hz, 2H, ABXY, 2 –CH_2–); 3.12 (dt, J_{HH} = 13.2 Hz, J_{PH} = 10.4 Hz, 2H, ABXY, 2 –CH_2–). ^{13}C NMR (125 MHz, $CDCl_3$, ppm): δ 205.4 (m, CO); 202.1 (m, CO); 144.5 (t, J_{CP} = 2.9 Hz, $C_{3,3'}$); 136.0 (t, J_{CP} = 20.0 Hz, *i*-Ph); 135.2 (t, J_{CP} = 19.6 Hz, *i*-Ph); 131.0 (t, J_{CP} = 6.1 Hz, *o*-Ph); 130.5 (t, J_{CP} = 6.0 Hz, *o*-Ph); 128.5 (s br, *p*-Ph); 128.2 (s, $C_{4,4'}$); 127.3 (t, J_{CP} = 4.6 Hz, *m*-Ph); 127.1 (t, J_{CP} = 4.6 Hz, *m*-Ph); 84.3 (m, $C_{2,2'}$); 74.2 (m, $C_{1,1'}$); 39.9 (t, J_{CP} = 19.8 Hz, 2 –CH_2–). ^{31}P NMR (121 MHz, $CDCl_3$, ppm): δ 43.2 (s br, 4P, 2 dppm). UV–Vis (CH_2Cl_2, nm): λ_{max} 579, 400 (sh) and 229. MS (FAB^+, *m/z*): 1361.0 [M^+]; 1333.1 [$M^+ - CO$]; 1277.2 [$M^+ - 3CO$]; 1137.0 [$M^+ - 8CO$].

2.7. X-ray crystallography

Green crystals of 2,5-[$Co_2(CO)_4$(dppm)$\{\mu_2$-η^2-$SiMe_3C_2\}]_2C_4H_2S$, **6**, are obtained by recrystallisation of the complex from CH_2Cl_2–hexane mixtures. A summary of selected crystallographic data for **6** is given in Table 3. Data were collected on a Nonius Kappa CCD diffractometer using graphite monochromated Mo Kα radiation (λ = 0.71073 Å). A combination of 1° ϕ and ω (with κ offsets) scans was used to collect sufficient data. The data frames were integrated and scaled using the DENZO-SMN package [17]. The structure was solved and refined using the SHELXTL/PC V5.1 package [18]. The structure was solved by direct methods and refinement was by full-matrix least-squares on F^2 using all data (negative intensities included). The H atom parameters were calculated and atoms were constrained as riding atoms with U isotropic 20% larger than the corresponding C-atoms for the phenyl H-atoms and 50% larger for the methyl H-atoms. Anisotropic thermal

parameters, hydrogen atom parameters and structure amplitudes are available as supplementary material. Table 4 contains selected bond distances and angles. Fig. 2 presents a molecular diagram of **6**. CCDC Reference No. 240985 (compound **6**).

3. Results and discussion

3.1. Synthesis and spectroscopic characterization

2,5-Bis(trimethylsilylethynyl)thiophene (**L**) was obtained in high yield (87%) by coupling reaction of 2,5-dibromothiophene with TMSA in the presence of $Pd(PPh_3)_4$ and CuI in triethylamine [16].

Complexes **1** and **2** have been obtained, as red and green unstable solids, by direct reaction between 2,5-bis(trimethylsilylethynyl)thiophene (**L**) and $Co_2(CO)_8$ in 1:1.5 and 1:2 ratios, respectively (Scheme 1).

In order to stabilise the dicobalt units by bridging effect between the two metal atoms, we have prepared complexes containing dppm or dppa ligands. Phosphine-substituted alkyne carbonyl complexes, 2-[$Co_2(CO)_4(\mu\text{-}X)\{\mu_2\text{-}\eta^2\text{-}SiMe_3C_2\}$]-5-($Me_3SiC{\equiv}C$)$C_4H_2S$ (X = dppa (**3**) or dppm (**4**)) and 2,5-[$Co_2(CO)_4(\mu\text{-}X)\{\mu_2\text{-}\eta^2\text{-}SiMe_3C_2\}]_2C_4H_2S$ (X = dppa (**5**) or dppm (**6**)), can be prepared by direct reaction between the alkyne and $Co_2(CO)_6(X)$ (X = dppa or dppm), under thermal conditions in a moderate yield (~30%) or by substitution reaction of carbonyl ligands in the presence of Me_3NO at the $Co_2(CO)_6$ units of complexes **1** and **2** (65% yield) (Scheme 1). This method, used previously in our laboratory for the syntheses of organometallic complexes with P-donor ligands [19], has clear advantages, namely, mild conditions, short reaction times and higher yields.

The FT-IR spectral changes of these reactions have been monitored until the $\nu_{C\equiv O}$ bands of the parent complex had disappeared. These changes suggest initial formation of monosubstituted intermediate products, which show five terminal stretching modes ν_{CO} (2059 (vs), 2024 (vs), 2003 (vs), 1979 (m) and 1959 (m)), in the characteristic range of analogous compounds where the ligand occupies an axial site [8,20]. This assumption is supported by the cleanness of the reactions as evidenced by the presence of isosbestic points in the successive spectra taken during the course of the reactions. This is followed by loss of CO and formation of the final product where the two P-atoms are coordinated to the Co atoms. The ^{31}P NMR data confirm the existence of these monosubstituted intermediate products; thus the spectrum presents two signals for both coordinated modes, monodentate and chelating phosphine (ca. 92.00 ppm (P_{coord}), 43.50 ppm (P_{free}) for dppa and ca. 35.00 ppm (P_{coord}), −21.81 ppm (P_{free}) for dppm).

Desilylation of **3** and **4** could be accomplished by treatment with Bu_4NF in THF/MeOH (10:1) (~20% yield) or with saturated KOH in degassed methanol (55%) to yield the terminal diyne compounds **7** and **8** as dark red solids. Complex **9** was only obtained when stronger desilylation conditions were used (Bu_4NF in THF/MeOH).

All these compounds have been characterized by analytical and spectroscopic data (IR, ^1H, $^1H\{^{31}P\}$, ^{13}C, ^{31}P NMR, MS and X-ray crystallography), details of which are given in Section 2. The IR spectra of **1** and **2** exhibit three strong absorptions in the carbonyl stretching region at 2088–2028 cm^{-1}; in dppm and dppa substituted complexes **3**–**9** these absorptions lie at lower frequencies 2029–1945 cm^{-1} and the spectral patterns are similar to those observed for previously reported cobalt-alkyne and cobalt-substituted-alkyne complexes [1c–1f,2c,7,8]. Complexes **1**, **3**, **4**, **7** and **8** contain uncomplexed C≡C triple bonds which give a $\nu_{C\equiv C}$ weak absorption between 2151 and 2095 cm^{-1} (as expected the $\nu_{C\equiv C}$ values of **7** and **8** are lower than **1**, **3** and **4**). In addition, desilylated compounds **7** and **8** exhibit a $\nu_{\equiv C-H}$ at ca. 3300 cm^{-1}.

The NMR spectroscopic data (^1H, ^{31}P and ^{13}C) for complexes **1**–**9** are consistent with overall geometry established in the solid state for complex **6** (Fig. 1), with the IR spectroscopy studies and with the proposed structures (Scheme 1).

In ^1H NMR spectra, the chemical shifts for the $SiMe_3$ and C≡CH protons are found to be very sensitive to cobalt complexation on the adjacent alkyne bond. As expected, the NMR spectra show a significant downfield shift for $SiMe_3$ and terminal protons in the Co_2-functionalized complexes **1**–**9** by ca. 0.15 and 2.5 ppm with respect to the free ligand, respectively, in accordance with the reduction in the C≡C triple-bond character [21]. In addition, the chemical shifts of the thiophene proton signals were consistent with the incorporation of 1 and 2 $Co_2(CO)_6$ or $Co_2(CO)_4(X)$ (X = dppa or dppm) units (see Section 2, Table 1). For all dppm-complexes the diastereotopic protons of $-CH_2-$ group are coupled with the two P-atoms, thus they appear as double triplet (Table 1, Fig. 1). For complex **9**, which contains a terminal alkyne proton, the –CH signal is coupled with the two chemically equivalent P-atoms and it appears as triplet with $^1H-^{31}P$ coupling constant of $J = 6.2$ Hz as in similar compounds [22]. The set of proton NMR signals, for all complexes, in the range δ 5.3–7.5 ppm evidences the presence of aromatic rings of the ligands (phenyl and thiophene).

The ^{31}P spectra, at room temperature, of all compounds **3**–**9** always show a broad singlet that is shifted to higher frequencies (ca. 35 and 92 ppm for dppm and dppa complex, respectively) with respect to the free ligands because of the coordination.

The ^{13}C NMR chemical shifts of the carbonyls in all the complexes appear as one or two signals at around δ 199 ppm or δ 202 and 206 ppm, respectively, suggesting

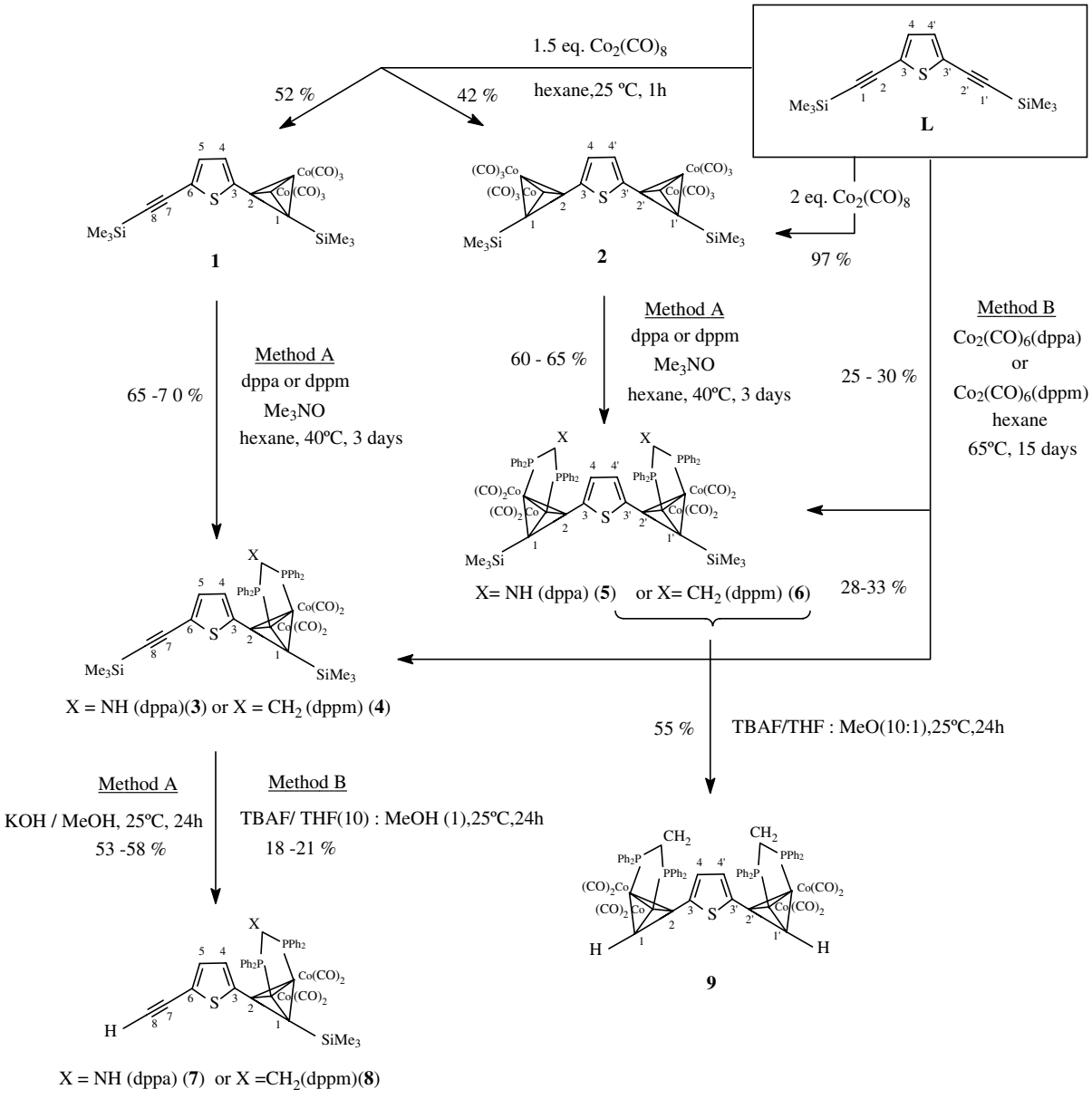

Scheme 1.

that they are rapidly interchanging on the NMR scale. The ^{13}C NMR resonances of the free and coordinated acetylene units were easily observed, and the chemical shifts of the carbon atoms are in the range of analogous complexes (δ 74–100 ppm) [1d,2c]. Thiophene carbons appear between δ 118–150 ppm (Table 2). The unambiguous assignment (see Section 2) of all carbon atoms has been carried out by using heteronuclear two-dimensional correlation spectroscopy (HMBC and HMQC).

All compounds gave satisfactory mass spectral data, thus the positive FAB mass spectra show the respective molecular ions or $M^+ - CO$, as well as peaks corresponding to the consecutive loss of the CO ligands.

The UV–Vis spectra of all complexes exhibit low intensity absorption bands with $\lambda_{max.}$ between 536 and 595 nm attributed to the d–d transitions. For complexes **2**, **5**, **6** and **9**, the presence of the second $Co_2(CO)_6$ or $Co_2(CO)_4X$ (X = dppa or dppm) unit resulted in a red shift in these absorption bands. In addition an intense absorption is observed at ca. 230 nm attributed to π–π* transition associated with the aromatic group.

3.2. X-ray crystallography

The single-crystal X-ray structure of complex **6** confirms the structure presented in Scheme 1. Complex **6** consists of a disubstituted thiophene ring with two bimetallic Co units at the 2 and 5 positions. Each bimetallic Co moiety has two terminal CO ligands on the Co atoms, bridging dppm ligands and bridging trimethylsilylethynyl

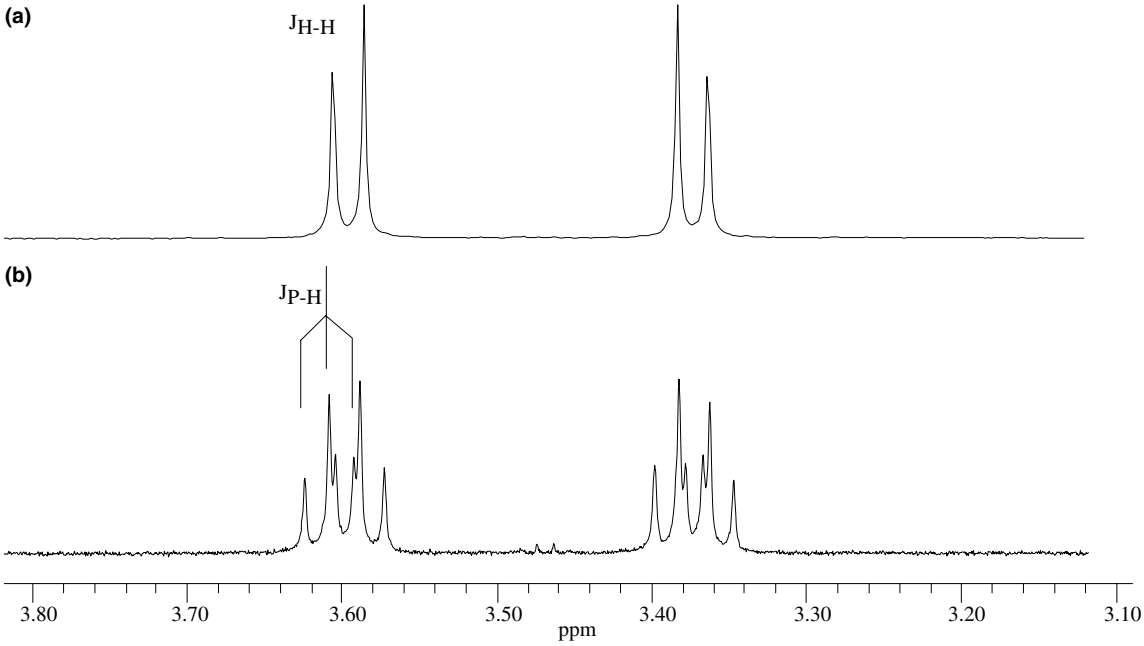

Fig. 1. (a) $^{1}H\{^{31}P\}$ NMR ($CDCl_3$) and (b) ^{1}H NMR ($CDCl_3$)spectra for complex **4**.

Table 1
Values of δ (^{1}H NMR, $CDCl_3$, ppm) to the compounds **1**–**9** and 2,5-bis(trimethylsilylethynyl)thiophene (**L**)

	H_4	H_5 or $H_{4'}$	–C≡C**H**	–C–C**H**	–C≡C**SiMe$_3$**	–C–C**SiMe$_3$**	>N**H**	>C**H$_2$**
L	7.04 (s) 7.06 (s)[a] 7.11 (d)	=H_4 =H_4 7.09 (d)	–	–	0.24 (s) 0.24 (s)[a] 0.24 (s)	– 0.39 (s)	–	–
1	J_{HH} = 3.9 Hz 7.13 (d)[a] J_{HH} = 3.8 Hz	J_{HH} = 3.9 Hz 7.11 (d)[a] J_{HH} = 3.8 Hz	–	–	0.24 (s)[a]	0.40 (s)[a]	–	–
2	7.15 (s)	=H_4	–	–	–	0.40 (s)	–	–
3	5.87 (d) J_{HH} = 3.8 Hz	6.60 (d) J_{HH} = 3.8 Hz	–	–	0.24 (s)	0.37 (s)	3.95 (t) J_{PH} = 6.4 Hz	–
4	6.46 (d) J_{HH} = 3.7 Hz	6.96 (d) J_{HH} = 3.7 Hz	–	–	0.26 (s)	0.36 (s)	–	3.60 (dt) 3.37 (dt)
5	5.26 (s)	=H_4	–	–	–	0.37 (s)	3.95 (t) J_{PH} = 6.5 Hz	–
6	6.56 (s)	=H_4	–	–	–	0.40 (s)	–	3.60 (dt) 3.47 (dt)
7	5.92 (d) J_{HH} = 3.8 Hz	6.64 (d) J_{HH} = 3.9 Hz	3.32 (s)	–	–	0.37 (s)	3.94 (t) J_{PH} = 6.3 Hz	–
8	6.51 (d) J_{HH} = 3.7 Hz	7.01 (d) J_{HH} = 3.7 Hz	3.37 (s)	–	–	0.37 (s)	–	3.60 (dt) 3.38 (dt)
9	7.14 (s)	=H_4	–	5.78 (t) J_{PH} = 6.2 Hz	–	–	–	3.56 (dt) 3.12 (dt)

[a] CD_2Cl_2.

Table 2
Values of δ (^{13}C NMR, $CDCl_3$, ppm) to the compounds **1**–**9** and 2,5-bis(trimethylsilylethynyl)thiophene (**L**)

	C_1	C_2	C_3	C_4	C_5 or $C_{4'}$	C_6 or $C_{3'}$	C_7 or $C_{2'}$	C_8 or $C_{1'}$
L	99.7 (s)	97.0 (s)	124.5 (s)	132.1 (s)	$=C_4$	$=C_3$	$=C_2$	$=C_1$
1	81.1 (s br)	93.3 (s br)	143.5 (s)	128.8 (s)	133.7 (s)	123.6 (s)	97.2 (s)	100.5 (s)
2	81.5 (s br)	94.1 (s br)	142.8 (s)	130.7 (s)	$=C_4$	$=C_3$	$=C_2$	$=C_1$
3	91.1 (m)	92.1 (m)	148.5 (t) J_{CP} = 4.3 Hz	128.5 (s)	133.2 (s)	120.7 (s)	98.9 (s) 98.6 (s)	
4	89.9 (m)	93.1 (m)	150.7 (t) J_{CP} = 3.8 Hz	126.0 (s)	133.2 (s)	121.0 (s)	98.7 (s) 98.2 (s)	
5	89.0 (m)	92.4 (m)	142.8 (m)	128.7 (s)	$=C_4$	$=C_3$	$=C_2$	$=C_1$
6	89.5 (t) J_{CP} = 9.8 Hz	93.5 (t) J_{CP} = 6.5 Hz	145.8 (t) J_{CP} = 2.9 Hz	127.2 (s)	$=C_4$	$=C_3$	$=C_2$	$=C_1$
7	91.1 (m)	91.9 (t) J_{CP} = 11.0 Hz	149.1 (t) J_{CP} = 3.8 Hz	128.1 (s)	133.5 (s)	119.5 (s)	78.2 (s)	81.1 (s)
8	91.1 (m)	93.0 (m)	150.0 (t) J_{CP} = 2.9 Hz	124.7 (s)	132.5 (s)	118.6 (s)	76.5 (s)	80.1 (s)
9	74.2 (m)	84.3 (m)	144.5 (t) J_{CP} = 2.9 Hz	128.2 (s)	$=C_4$	$=C_3$	$=C_2$	$=C_1$

ligands. The geometric parameters for **6** have been summarized in Table 3. Table 4 contains selected bond distances and angles, Fig. 2 presents a view of the molecule with the atom-labelling scheme and Fig. 3 is the extended structure of **6**.

Complex **6** crystallizes in the monoclinic space group $P2_1/c$, with one molecule in the asymmetric unit. The structure also contains one molecule of chloroform that is grossly disordered, which could not be modeled satisfactorily. The contribution from this solvent molecule was removed from the observed data using SQUEEZE in the software program PLATON, but the atom count from the $CHCl_3$ is included in the empirical formula [23]. Although the complex does not contain any crystallographic symmetry, the molecule is symmetric about a mirror plane through the thiophene moiety, the bond lengths are sufficiently comparable such that discussion will be confined to one half of the molecule. A highly distorted tetrahedron is formed by the coordination of the dicobalt units with the ethynyl carbons, with a Co(1)–Co(2) bond length of 2.504(1) Å, and the average Co–C bond length was determined to be 1.971(1) Å. Comparable Co–Co distances of 2.4892(4) and 2.4906(4) Å are reported for the related compound $\{(Co_2(CO)_4dppm)(\mu_2\text{-}\eta^2\text{-}SiMe_3C_2)\}_2(SiMe_3C{\equiv}C)(1,3,5\text{-}C_6H_3)$ [7]. The distance between the two Co_2 moieties was found to be 8.26 Å, which was calculated by placing a centroid between Co(1) and Co(2), and similarly Co(3) and Co(4), and then determining the distance

Table 3
Crystal data and structure refinement for compound **6**

Empirical formula	$C_{73}H_{65}Cl_3Co_4O_8P_4SSi_2$
Formula weight	1624.44
Temperature	297(2) K
Wavelength	0.71073 Å
Crystal system	$P2(1)/c$
Space group	Monoclinic
Unit cell dimensions	
a	12.1439(2) Å
b	12.5980(2) Å
c	52.5016(8) Å
α	90°
β	91.441(9)°
γ	90°
V	8029.6(2) Å^3
Z	4
$D_{calc.}$	1.344 Mg/m^3
Absorption coefficient	1.096 mm^{-1}
$F(000)$	3320
Crystal size	$0.10 \times 0.07 \times 0.04$ mm^3
θ range for data collection	0.78–25.79°
Index ranges	$-14 \leqslant h \leqslant 14$, $-15 \leqslant k \leqslant 15$, $-63 \leqslant l \leqslant 62$
Reflections collected	49454
Independent reflections	14832 [R_{int} = 0.0728]
Completeness to θ = 25.79°	96.0%
Max. and min. transmission	0.9575 and 0.8983
Refinement method	Full-matrix least-squares on F^2
Data/restraints/parameters	14832/0/826
Goodness-of-fit on F^2	0.947
Final R indices [$I > 2\sigma(I)$]	R_1 = 0.0716, wR_2 = 0.1797
R indices (all data)	R_1 = 0.1254, wR_2 = 0.2009
Largest diff. peak and hole	0.630 and −0.581 e Å^{-3}

Table 4
Selected bond distances (Å) and angles (°) for **6**

Co(1)–Co(2)	2.504(1)	Co(3)–Co(4)	2.493(1)
Co(1)–C(6)	1.958(6)	Co(3)–C(40)	1.978(6)
Co(1)–C(5)	1.993(5)	Co(3)–C(39)	2.006(5)
Co(1)–C(7)	1.755(9)	Co(3)–C(41)	1.765(7)
Co(1)–C(8)	1.792(7)	Co(3)–C(42)	1.786(8)
Co(2)–C(5)	1.949(5)	Co(4)–C(39)	1.945(5)
Co(2)–C(6)	1.985(6)	Co(4)–C(40)	1.973(5)
Co(2)–C(9)	1.791(7)	Co(4)–C(43)	1.768(8)
Co(2)–C(10)	1.778(8)	Co(4)–C(44)	1.804(7)
Co(1)–P(1)	2.227(2)	Co(3)–P(3)	2.222(2)
Co(2)–P(2)	2.211(2)	Co(4)–P(4)	2.220(2)
Si(1)–C(6)	1.857(6)	Si(2)–C(40)	1.834(6)
C(7)–Co(1)–C(8)	101.2(3)	C(41)–Co(3)–C(42)	101.3(3)
C(7)–Co(1)–C(6)	101.9(3)	C(41)–Co(3)–C(40)	103.0(3)
C(8)–Co(1)–C(6)	103.3(3)	C(42)–Co(3)–C(40)	99.9(3)
C(7)–Co(1)–C(5)	101.3(3)	C(41)–Co(3)–C(39)	103.0(3)
C(8)–Co(1)–C(5)	140.1(3)	C(42)–Co(3)–C(39)	137.2(3)
C(6)–Co(1)–C(5)	39.7(2)	C(40)–Co(3)–C(39)	40.4(2)
C(7)–Co(1)–P(1)	97.5(2)	C(41)–Co(3)–P(3)	97.5(2)
C(8)–Co(1)–P(1)	105.8(2)	C(42)–Co(3)–P(3)	110.2(2)
C(6)–Co(1)–P(1)	140.8(2)	C(40)–Co(3)–P(3)	139.2(2)
C(5)–Co(1)–P(1)	103.3(2)	C(39)–Co(3)–P(3)	100.9(2)
C(7)–Co(1)–Co(2)	149.6(2)	C(41)–Co(3)–Co(4)	151.0(2)
C(8)–Co(1)–Co(2)	99.0(2)	C(42)–Co(3)–Co(4)	96.3(3)
C(6)–Co(1)–Co(2)	51.1(2)	C(40)–Co(3)–Co(4)	50.8(2)
C(5)–Co(1)–Co(2)	49.8(2)	C(39)–Co(3)–Co(4)	49.8(1)
P(1)–Co(1)–Co(2)	98.48(6)	P(3)–Co(3)–Co(4)	97.88(5)
C(10)–Co(2)–C(9)	101.1(3)	C(43)–Co(4)–C(44)	100.1(3)
C(10)–Co(2)–C(5)	97.6(3)	C(43)–Co(4)–C(39)	97.5(3)
C(9)–Co(2)–C(5)	140.1(3)	C(44)–Co(4)–C(39)	143.8(3)
C(10)–Co(2)–C(6)	105.0(3)	C(43)–Co(4)–C(40)	101.9(3)
C(9)–Co(2)–C(6)	100.9(3)	C(44)–Co(4)–C(40)	104.0(3)
C(5)–Co(2)–C(6)	39.8(2)	C(39)–Co(4)–C(40)	41.1(2)
C(10)–Co(2)–P(2)	98.5(2)	C(43)–Co(4)–P(4)	99.8(2)
C(9)–Co(2)–P(2)	107.3(2)	C(44)–Co(4)–P(4)	106.1(2)
C(5)–Co(2)–P(2)	104.4(2)	C(39)–Co(4)–P(4)	101.7(2)
C(6)–Co(2)–P(2)	138.8(2)	C(40)–Co(4)–P(4)	138.8(2)
C(10)–Co(2)–Co(1)	148.7(2)	C(43)–Co(4)–Co(3)	148.4(2)
C(9)–Co(2)–Co(1)	102.3(2)	C(44)–Co(4)–Co(3)	102.3(3)
C(5)–Co(2)–Co(1)	51.3(2)	C(39)–Co(4)–Co(3)	52.0(2)
C(6)–Co(2)–Co(1)	50.1(2)	C(40)–Co(4)–Co(3)	51.0(2)
P(2)–Co(2)–Co(1)	94.14(5)	P(4)–Co(4)–Co(3)	95.15(5)
P(1)–C(14)–P(2)	110.0(3)	P(1)–C(14)–P(2)	110.0(3)

between the two centroids which spans across the thiophene ring.

The coordination geometry of each Co is similar to a pyramid with a pentagonal-shaped base, where the Co is in the centre of the pyramid. The distortion of the pyramid is due to the constrained tetrahedron comprised of Co(1)–Co(2)–C(5)–C(6), as well as the bridging of the dppm ligand. The carbonyl moieties coordinate to the Co atoms in the least sterically hindered sites, thus making up the pyramid. The apex of the pyramid is one of the carbonyl groups, and the base is comprised of the other carbonyl group, one of the phosphorus atoms of the dppm ligand, the two ethynyl carbons, and the other Co atom. The bond lengths of the apex carbonyls to the Co atoms, C(8)–Co(1) and C(9)–Co(2), are 1.792(7) and 1.791(7) Å, respectively. These bond lengths are not statistically different from the base carbonyls to Co atoms, which are 1.755(9) and 1.778(8) Å, for C(7)–Co(1) and C(10)–Co(2), respectively. The dihedral angle comprised of Co(2)–C(5)–C(6)–Co(1) was determined to be −84.9(2)°, whereas the dihedral angle comprised of C(5)–Co(2)–Co(1)–C(6) was determined to be −52.2(3)°. The analogous dihedral angle of P(2)–Co(2)–Co(1)–P(1) was determined to be −4.90(6)°, thus suggesting a greater strain on the dicobalt units by the coordination of the ethynyl carbons compared to the bridging of the dppm ligand. The bite angle of the dppm ligand was found to be 110.0(3)°, which is consistent to analogous bite angles of dppm on Co–Co complexes [24]. The C(5)–C(6) bond length of the bridging ethynyl ligand is 1.341(7) Å, which is consistent with reported dicobalt ethynyl complexes [25].

The bond lengths of the Co atoms to the phosphorus atoms of the dppm ligand are 2.227(2) Å and 2.211(2) Å for Co(1)–P(1) and Co(2)–P(2), respectively. The Co–P bond lengths of the same dppm are statistically different; however, no chemical significance is ascribed to the

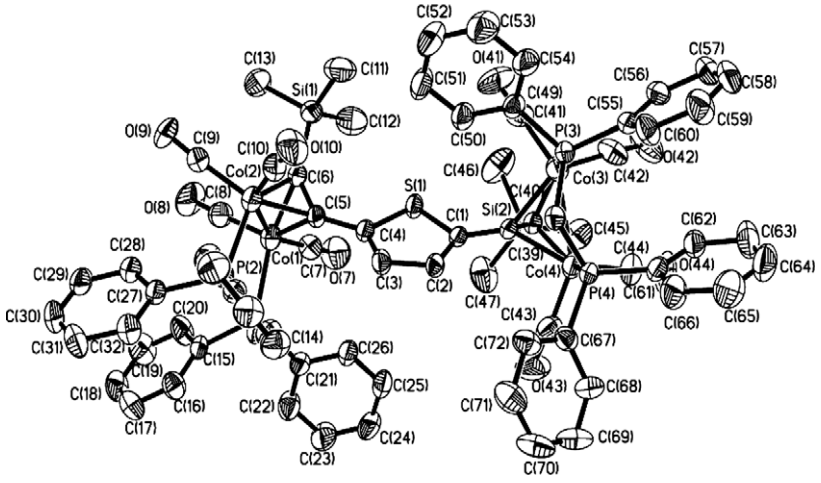

Fig. 2. ORTEP diagram of **6**, with 35% ellipsoids. Hydrogen atoms have been removed for clarity.

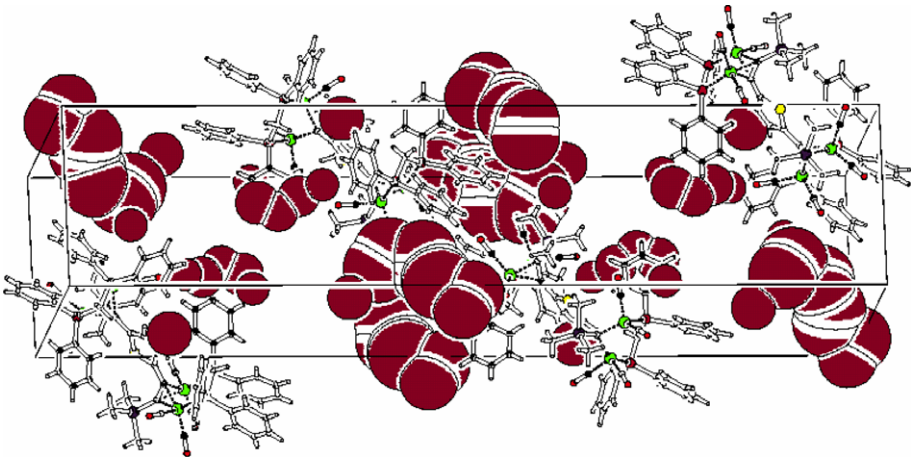

Fig. 3. Extended structure of **6** showing cavities where the contribution from grossly disordered chloroform solvent molecules occupied.

difference. The phenyl rings on the dppm ligand are oriented in a fashion such that the rings twist in the same direction with respect to each other in order to minimize steric crowding. The average carbonyl C≡O bond length was determined to be 1.138(2) Å, where all of the bond lengths were sufficiently similar (differences between the bond lengths were below 1σ). The thiophene ring is essentially planar with a root mean square deviation of 0.0032 Å. There does not appear to be any intramolecular hydrogen bonding within the molecule.

3.3. Electrochemical studies

Table 5 summarizes data of $E_{1/2}$ for the electrochemical oxidation and reduction of compounds **1**–**9**. The ligand **L** does not present any oxidation or reduction peaks in the potential range between −1.8 V and +1.6 V vs. Fc^{*+}/Fc^{*} (Fc* = decamethylferrocene) in CH_2Cl_2 and THF solution.

3.3.1. Electrochemistry of *1*–*2*

The cyclic and square-wave voltammetry (CV and SWV, respectively) in CH_2Cl_2 solution of the $Co_2(CO)_6C_2$ derivative **1** at room temperature show a completely irreversible reduction wave at $E_p = -1.05$ V vs. Fc^{*+}/Fc^{*} (SWV) and at $E_{pc} = -1.14$ V (CV, at a sweep rate $v = 0.1$ V s^{-1}). Upon scan reversal in CV, no coupled anodic peak is observed, but a new irreversible peak at +0.12 V appears. This behaviour resembles other related $Co_2(CO)_6$(alkyne) derivatives [6d,7,8,26–29] and indicates that a monoelectronic reduction process is followed by the fast decomposition of the radical anion $\mathbf{1}^-$ in a variety of fragments (EC mechanism) including $Co(CO)_4^-$, which is oxidised at 0.12 V. At −30 °C, the chemical disintegration of $\mathbf{1}^-$ is much slower, as the CV shows a quasi-reversible reduction wave ($i_{pa}/i_{pc} \approx 0.6$ at 0.1 V s^{-1}, $E_{1/2} = -1.01$ V) and the diminution of the peak at 0.12 V; however, other new small anodic peaks can be observed at −0.61 and −0.44 V (Fig. 4(a)).

The oxidation of **1** in CH_2Cl_2 is chemically irreversible at room temperature and at 0.1 V s^{-1} ($E_{pa} = 1.27$ V) but, as the sweep rate increases, a coupled cathodic peak can be gradually observed, indicative of an EC process ($i_{pc}/i_{pa} \approx 0.55$ at 2 V s^{-1}). Accordingly, sweeps at −30 °C (Fig. 4(b)) show a partially chemically reversible wave ($i_{pc}/i_{pa} \approx 0.55$ at 0.1 V s^{-1}). The chemical reaction following the oxidation to $\mathbf{1}^+$ leads to a strong

Table 5
Electrochemical data for **1**–**9**[a]

	$E_{1/2}$ for reduction	$\Delta E_{1/2}$ (red)	$E_{1/2}$ for oxidation	$\Delta E_{1/2}$ (ox)
1	−1.01[b]		1.23[b]	
2	−0.97[b]; −1.08[b]	0.11[b]	1.13[b] ; 1.37[b]	0.24
3	−1.51[b]		0.61 (*0.61*)	
4	−1.58[b] (*−1.65*)		0.67 (*0.66*)	
5	−1.55[b]; −1.67[b] (*−1.68*[b]); (*−1.84*[b])	0.12[b] (*0.16*[b])	0.47; 0.76 (*0.44*); (*0.72*)	0.29 (*0.28*)
6	−1.55[b]; −1.68[b]	0.13[b]	0.54, 0.83	0.29
7	−1.50		0.63	
8	−1.53[b]		0.69	
9	−1.53[b]; −1.66[b]	0.13[b]	0.50; 0.70	0.20

[a] In V vs. Fc^{*+}/Fc^{*} in CH_2Cl_2 solution (values in italics are in THF solution). Data are taken from CV and SWV at 25 °C unless otherwise stated.
[b] From CV and SWV at −30 °C.

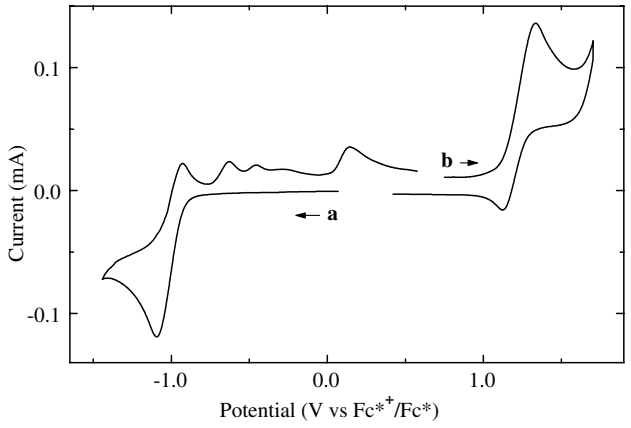

Fig. 4. Cyclic voltammograms for the reduction (a) and oxidation (b) of a solution of **1** in CH_2Cl_2 containing 0.2 M $TBAPF_6$ at 0.1 V s^{-1} and −30 °C. Glassy carbon working electrode.

contamination of the electrode surface (Pt and glassy carbon) by an adsorbed substance that is reduced in a subsequent negative cycle at ca. −0.7 V. The result of this reduction is a new adsorbed product that is oxidized at ca. 0.55 V. This behaviour has also been found in this laboratory with other related derivatives, like *x*-[$Co_2(CO)_6\{\mu_2$-η^2-$SiMe_3C_2\}$]-*y*-$(Me_3SiC{\equiv}C)C_4H_2S$, ($x = 2$, 3 and $y = 4$; $x = 2$ and $y = 3$) and even the simple $Co_2(CO)_6\{\mu_2$-η^2-$SiMe_3C_2H\}$ [30]. The product of the reduction at ca. −0.7 V must be adsorbed cobalt (0), which is desorbed by oxidation at ca. +0.55 V, as the same anodic desorption peak is obtained from a solution of $CoCl_2$ after its reduction.

The reduction of **2**, which contains two equivalent $C_2Co_2(CO)_6$ redox centres, is irreversible at 25 °C ($E_{pc} = -1.05$ V at 0.1 V s^{-1}), but two distinct peaks are observed in SWV. At −30 °C, CV shows two peaks with coupled anodic ones, indicating enhanced chemical reversibility. Therefore, the stability of the $\mathbf{2}^-$ anion obtained in the first reduction process is much higher than that observed in other related complexes [29–32], but equivalent to that found in this laboratory for $\{(Co_2(CO)_6)\mu_2$-η^2-$SiMe_3C_2\}_2(SiMe_3C{\equiv}C)(1,3,5\text{-}C_6H_3)$ [7]. The CV oxidation of **2** in CH_2Cl_2 leads to two quasi-reversible waves at 25 °C which are almost completely reversible at −30 °C. Table 5 assembles $E_{1/2}$ values.

It is noteworthy that very few studies can be found in the literature on the oxidation of $Co_2(CO)_6$(alkyne) derivatives. Wong et al. [1e] reported the reduction of the complex 5,5′-[$\{Co_2(CO)_6\}\{\mu_2$-η^2-$SiMe_3C_2\}$]$_2$-2,2′-$(C_4H_2S)_2$ in CH_2Cl_2, which takes place irreversibly at −1.58 V vs. the ferrocene (Fc) couple (−1.03 V vs. Fc^{*+}/Fc^*, see Section 2) at room temperature. They observed an anodic peak at 0.71 V vs. Fc^+/Fc (1.26 V vs. Fc^{*+}/Fc^*) which was assigned to the oxidation of $[Co(CO)_4^-]$ resulting from the decomposition of the electrogenerated monoanion. However, this potential value is far too positive for $[Co(CO)_4^-]$; when CV is performed to a solution of $Co_2(CO)_8$ in CH_2Cl_2, an irreversible reduction peak is observed at −0.52 V and, upon scan reversal, $[Co(CO)_4^-]$ oxidation takes place at +0.12 V (measurement in our laboratory). Furthermore, Wong et al. performed experiments at −78 °C, where the chemical reaction following reduction of their complex was completely quenched and, correspondingly, found two reversible reduction peaks. In this latter case, they still found the oxidation peak, now at +0.66 V vs. Fc^+/Fc (1.21 V vs. Fc^{*+}/Fc^*). All this data indicate that the anodic peak corresponds to the oxidation of the original complex 5,5′-[$\{Co_2(CO)_6\}\{\mu_2$-η^2-$SiMe_3C_2\}$]$_2$-2,2′-$(C_4H_2S)_2$, which takes place at a potential value quite similar to **2**.

Jung et al. [6d] have studied some closely related complexes, 2,5-[$Co_2(CO)_6\{\mu_2$-η^2-$RC_2\}$]$_2(C_4H_2S)$ (R = n-butyl, phenyl), but only at room temperature, where they found irreversible waves both for reduction and oxidation. The potential values reported are consistent with our data for **2**.

The appearance of two different reduction and oxidation peaks for **2** and not of a single bielectronic wave in each case indicates the existence of interaction between the redox centres through the thiophene ligand. The separation between the different peaks ($\Delta E_{1/2}$) is a measure of the magnitude of this effect and, for **2** corresponds to class II systems in the Hush–Robin–Day classification of mixed-valence compounds (systems with low-moderate electronic delocalization) [5d,33].

3.3.2. Electrochemistry of 3–9

The coordination of dppm or dppa phosphorous ligands to the Co_2C_2 core increases its electron density and facilitates oxidation, whereas it is necessary to apply potentials 0.5 – 0.6 V more negative than in **1**–**2** to achieve reduction. The chelating phosphine ligands also contribute to the stabilization of the Co–Co bond, increasing the lifetimes of the radical anions and cations.

In the room temperature CV and SWV oxidation of **3**, **4**, **7** and **8**, one chemically reversible wave is obtained with $i_{pc}/i_{pa} = 1$ in the 0.02–10 V s^{-1} range of CV sweep rates (Fig. 5, Table 5). Thus, $\mathbf{3}^+$, $\mathbf{4}^+$, $\mathbf{7}^+$ and $\mathbf{8}^+$ are chemically stable under the actual conditions of the experiment. $E_{1/2}$ in CH_2Cl_2 is ca. 0.62 V and ca. 0.56 V less positive than for **1** for the dppa- and dppm-substituted complexes, respectively. This 0.06 V difference between the derivatives of the two different phosphine ligands has also been observed for $Co_2(CO)_4L(\mu_2$-η^2-$Me_3SiC_2C{\equiv}CSiMe_3)$, where L is dppa or dppm [8].

The CV and SWV reduction of **3**, **4**, **7** and **8** at 25 °C takes place at a very negative potential, and a single, partially chemically reversible peak is obtained in CH_2Cl_2 (Fig. 6(a)). i_{pa}/i_{pc} increases with v at room temperature, whereas almost complete chemical reversibility is attained at −30 °C (for **3**, $i_{pa}/i_{pc} = 1$ even at a sweep rate as slow as 0.02 V s^{-1}, Fig. 6(b)), indicating that

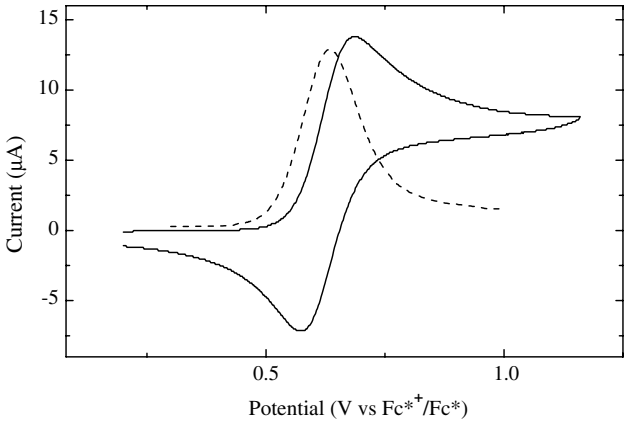

Fig. 5. Cyclic (—) and square wave (– – –) voltammograms for the oxidation of **7** in CH_2Cl_2 containing 0.2 M $TBAPF_6$ at 25 °C. CV: $v = 0.1$ V s^{-1}. SWV: scan increment = 2 mV, SW amplitude = 25 mV; frequency = 60 Hz. Pt working electrode.

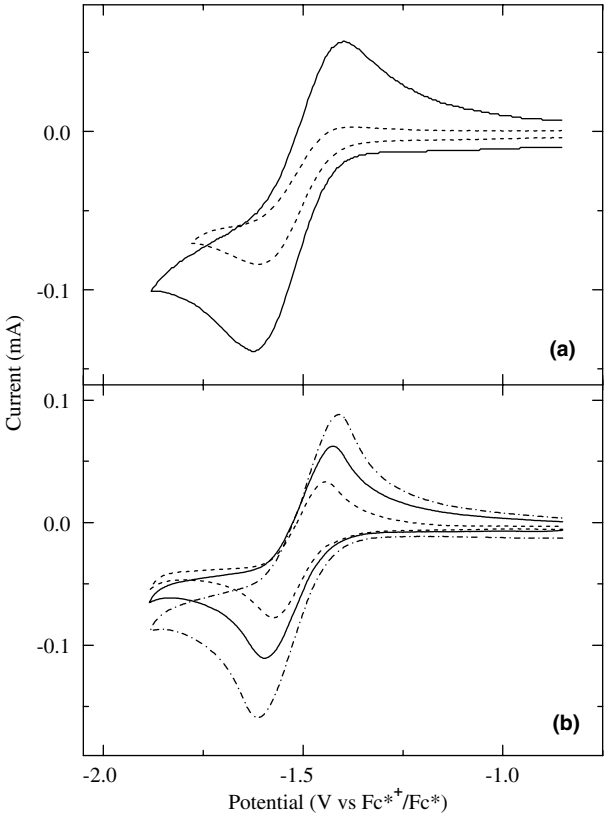

Fig. 6. Cyclic voltammograms for the reduction of **3** in CH_2Cl_2 containing 0.2 M $TBAPF_6$ at 0.1 V s^{-1}. (a) At room temperature on a Pt working electrode; 0.2 V s^{-1} (– – –), 0.5 V s^{-1} (—). (b) At −30 °C on a glassy carbon working electrode; 0.02 V s^{-1} (- - -), 0.05 V s^{-1} (—), 0.1 V s^{-1} (-·-·-).

the stabilising effect of the chelating dppm and dppa ligands makes the fragmentation of $\mathbf{3}^-$, $\mathbf{4}^-$, $\mathbf{7}^-$ and $\mathbf{8}^-$ much slower than for the parent $\mathbf{1}^-$. The reduction of complex **4** was also performed in THF solution; in this solvent, complete chemical reversibility is observed at 25 °C even at $v = 0.1$ V s^{-1}. The shift in $E_{1/2}$ upon dppm or dppa coordination (between 0.50 and 0.57 V, see Table 5) and the increased lifetime of the radical anions are consistent with reported data [31,34,35]. It is noteworthy that the dppa derivatives **3** and **7** which, as above mentioned, are easier to oxidize, also have the less negative reduction potentials. This behaviour was also observed for related compounds [8].

The electrochemical oxidation of **5**, **6** and **9** shows two sequential reversible waves at 25 °C both in CV ($i_{pa}/i_{pc} = 1$ in the 0.02–10 V s^{-1} range) and SWV (Fig. 7). Correspondingly, the CV and SWV reduction of **5** and **6** displays two distinct waves at −30 °C, which are completely reversible at this low temperature (Fig. 8). On the other hand, for the reduction of **9** two peaks are only distinguished in SWV at −30 °C (an irreversible complex peak is observed in CV). $E_{1/2}$ values are assembled in Table 5.

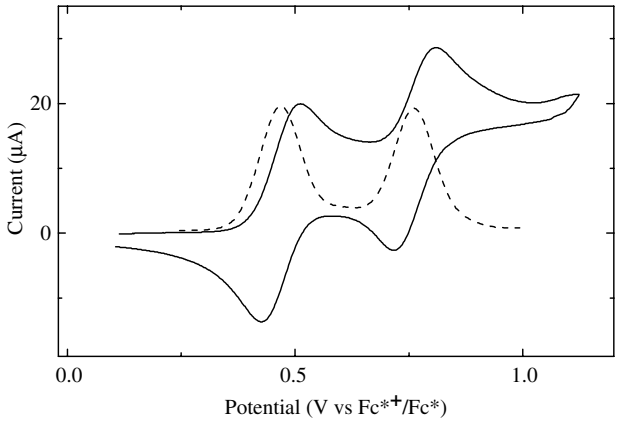

Fig. 7. Cyclic (—) and square wave (– – –) voltammograms for the oxidation of **5** in CH_2Cl_2 containing 0.2 M $TBAPF_6$ at 25 °C. CV: $v = 0.1$ V s^{-1}. SWV: scan increment = 2 mV, SW amplitude = 25 mV; frequency = 30 Hz. Pt working electrode.

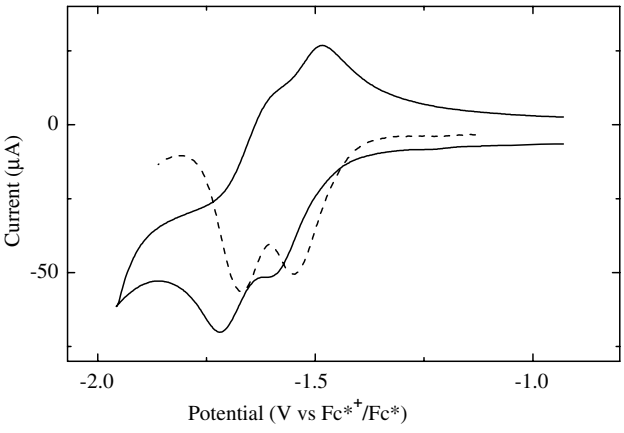

Fig. 8. Cyclic (—) and square wave (– – –) voltammograms for the reduction of **5** in CH_2Cl_2 containing 0.2 M $TBAPF_6$ at −30 °C. CV: $v = 0.1$ V s^{-1}. SWV: scan increment = 2 mV, SW amplitude = 25 mV; frequency = 30 Hz. Glassy carbon working electrode.

From the oxidation waves, $\Delta E_{1/2}$ is 0.29 V in **5** and **6** and 0.20 V in **9**, a bigger value than that obtained from the reduction processes ($\Delta E_{1/2}$ = 0.12–0.13 V). Differences in $\Delta E_{1/2}$ for oxidations and reductions are not unusual [31,36], as different MOs are involved in each process and through-bond interactions dominate through-space ones in these systems with a π-delocalised spacer [10f]. Both $\Delta E_{1/2}$ are in the range corresponding to class II mixed-valence compounds, and it can be concluded that there is low-moderate interaction between the two equivalent organometallic redox centres in **5**, **6** and **9**.

Acknowledgements

We express our great appreciation to the Dirección General de Investigación Científica y Tecnológica (Grant No. BQU2002-02522), Spain. X-ray diffraction data were collected at the Monocrystal Diffraction Laboratory SidI, Facultad de Ciencias, Universidad Autónoma de Madrid, Spain.

Appendix A. Supplementary material

Supplementary data associated with this article can be found, in the online version, at doi:10.1016/j.jorganchem.2004.07.028.

References

[1] (a) A. Sappa, A. Tiripicchio, P. Braunstein, Chem. Rev. 83 (1983) 203;
(b) P.R. Raithby, M.J. Rosales, Adv. Inorg. Chem. Radiochem. 29 (1985) 169;
(c) R.S. Dickinson, P.J. Fraser, in: F.G.A. Stone, R. West (Eds.), Advances in Organometallic Chemistry, vol. 12, 1974, p. 323;
(d) B. Happ, T. Bartik, C. Zucchi, M.C. Rossi, F. Ghelfi, G. Pályi, G. Váradi, G. Szalontai, I.T. Horváth, A. Chiesi-Villa, C. Guastini, Organometallics 14 (1995) 809;
(e) W.-Y. Wong, H.-Y. Lam, S.-M. Lee, J. Organomet. Chem. 595 (2000) 70;
(f) B.H. Danna, B.H. Robinson, J. Simpson, J. Organomet. Chem. 648 (2002) 251;
(g) N.J. Long, C.K. Williams, Angew. Chem. Int. Ed. Engl. 42 (2003) 2586;
(h) P.J. Low, M.I. Bruce, in: F.G.A. Stone, R. West (Eds.), Advances in Organometallic Chemistry, 48, 2002, p. 71;
(i) F.-E. Hong, Y.-C. Chang, R.-E. Chang, S.-C. Chen, B.-T. Ko, Organometallics 21 (2002) 961.

[2] (a) F. Diederich, Y. Rubin, Angew. Chem. Int. Ed. Eng. 104 (1992) 1123;
(b) Y. Rubin, C.B. Knobler, F. Diederich, J. Am. Chem. Soc. 112 (1990) 4966;
(c) F. Diederich, Y. Rubin, O.L. Chapman, S.N.S. Goroff, Helv. Chim. Acta 77 (1994) 1441;
(d) T. Rappert, O. Nürnberg, H. Werner, Organometallics 12 (1993) 1359;
(e) H. Werner, O. Gevert, P. Steinert, J. Wolf, Organometallics 14 (1995) 1786;
(f) J. Lewis, B. Lin, M.S. Khan, M.R.A. Al-Mandhary, P.R. Raithby, J. Organomet. Chem. 484 (1994) 161.

[3] (a) M.L.H. Green, S.R. Marder, M.E. Thomson, J.A. Bandy, D. Bloor, P.V. Kolomsky, R.J. Jones, Nature 330 (1987) 360;
(b) A.D. Hunter, Organometallics 8 (1989) 1118;
(c) R. Chukwu, A.D. Hunter, B.D. Santarsiero, Organometallics 11 (1992) 589;
(d) Z. Yuan, N.J. Taylor, Y. Sun, T.B. Marder, I.D. Williams, J.T. Cheng, J. Organomet. Chem. 449 (1993) 27;
(e) J.S. Miller, A.J. Epstein, Angew. Chem. Int. Ed. Engl. 33 (1994) 385;
(f) M.S. Khan, M.R.A. Al-Mandhary, M.K. Al-Suti, B. Ahrens, M.F. Mahon, L. Male, P.R. Raithby, C.E. Boothby, A. Köhler, J. Chem. Soc., Dalton Trans. (2003) 74;
(g) V.W.-W. Yam, K.-L. Cheuhg, E.C.-C. Cheng, N. Zhu, K.-K. Cheung, J. Chem. Soc., Dalton Trans. (2003) 1830;
(h) S.K. Hurst, M.G. Humphrey, J.P. Morrall, M.P. Cifuentes, M. Samoc, B.L. Davies, G.A. Heath, A.C. Willis, J. Organomet. Chem. 670 (1-2) (2003) 56;
(i) I.S. Le, D.M. Shin, Y. Yoon, S.M. Shin, Y.K. Chung, Inorg. Chim. Acta 343 (2003) 41;
(j) V.W.-W. Yam, K.M.-C. Wong, N. Zhu, Angew. Chem. Int. Ed. Eng. 42 (2003) 1400.

[4] (a) S. Creager, C.J. Yu, C. Bamdad, S. O'Connor, T. Maclean, E. Lam, Y. Chong, G.T. Olsen, J. Luo, M. Gozon, J.F. Hayyem, J. Am. Chem. Soc. 121 (1999) 1059;
(b) P. Stepnicka, R. Gyepes, I. Císarova, Organometallics 18 (1999) 627;
(c) P.I. Dosa, C. Erben, V.S. Iyer, K.P.C. Vollhardt, I.M. Wasser, J. Am. Chem. Soc. 121 (1999) 10430;
(d) D.T. McQuade, A.E. Pullen, T.M. Swager, Chem. Rev. 100 (2000) 2537;
(e) N. Robertson, C.A. McGowan, Chem. Soc. Rev. 32 (2003) 96.

[5] (a) Molecular and Biomolecular Electronics, R.R. Birge (Ed.), Advances in Chemistry Series, 240, American Chemical Society, 1991;
(b) W.P. Kirk, M.A. Reed (Eds.), Nanostructures and Mesoscopic Systems, Academic, New York, 1992;
(c) A. Aviram (Ed.), Molecular Electronics: Science and Technology, Confer. Proc. No. 262, American Institute of Physics, New York, 1992;
(d) D. Astruc, Electron Transfer and Radical Processes in Transition-Metal Chemistry, VCH Publishers, New York, 1995;
(e) M.D. Ward, Chem. Soc. Rev. 24 (1995) 121;
(f) R.P. Andres, J.D. Bielefeld, J.I. Henderson, D.B. Janes, V.R. Kolagunta, C.P. Kubiak, W.J. Mahoney, R.G. Osifchin, Science 273 (1996) 1690;
(g) V. Grosshenny, A. Harriman, M. Hissler, R. Ziessel, Plat. Met. Rev. 40 (1996) 26;
(h) V. Grosshenny, A. Harriman, M. Hissler, R. Ziessel, Plat. Met. Rev. 40 (1996) 72;
(i) S. Barlow, D. O'Hare, Chem. Rev. 97 (1997) 637;
(j) D. Feldheim, C.D. Keating, Chem. Soc. Rev. 27 (1998) 1;
(k) F. Paul, C. Lapinte, Coord. Chem. Rev. 431 (1998) 178;
(l) C.P. Collier, E.W. Wong, M. Belohradsky, F.M. Raymo, J.F. Stoddart, P.J. Kuekes, R.S. Williams, J.R. Heath, Science 285 (1999) 391;
(m) S. Kheradmandan, K. Heinze, H.W. Schmalle, H. Berke, Angew. Chem. Int. Ed. Eng. 38 (1999) 2270.

[6] (a) N. Le Narvor, L. Toupet, C. Lapinte, J. Am. Chem. Soc. 117 (1995) 7129;
(b) T. Bartik, B. Bartik, R. Dembinski, J.A. Gladysz, Angew. Chem. Int. Ed. Engl. 35 (1996) 414;
(c) F. Coat, C. Lapinte, Organometallics 15 (1996) 477;
(d) T.S. Jung, J.H. Kim, E.K. Jang, D.H. Kim, Y.-B. Sim, B.

Park, S.C. Shin, J. Organomet. Chem. 599 (2000) 232;
(e) R.D. Adams, B. Qu, Organometallics 19 (2000) 2411;
(f) H.J. Jiao, J.A. Gladysz, New.J. Chem. 25 (2001) 551.
[7] (a) C. Moreno, M.L. Marcos, G. Domínguez, A. Arnanz, D.H. Farrar, R. Teeple, A. Lough, J. González-Velasco, S. Delgado, J. Organomet. Chem. 631 (2001) 19;
(b) R.M. Medina, C. Moreno, M.L. Marcos, J.A. Castro, F. Benito, A. Arnanz, S. Delgado, J. González-Velasco, M.J. Macazaga, Inorg. Chim. Acta 357 (2004) 2069.
[8] M.L. Marcos, M.J. Macazaga, R.M. Medina, C. Moreno, J.A. Castro, J.L. Gómez, S. Delgado, J. González-Velasco, Inorg. Chim. Acta 312 (2001) 249.
[9] (a) J. Roncali, Chem. Rev. 97 (1997) 173;
(b) D.T. McQuade, A.E. Pullen, T.M. Swager, Chem. Rev. 100 (2000) 2537;
(c) C.J. Elsevier, J. Reedijk, P.H. Walton, M.D. Ward, J. Chem. Soc., Dalton Trans. (2003) 1869.
[10] (a) G.H. Worth, B.H. Robinson, J. Simpson, Appl. Organomet. Chem. 4 (1990) 481;
(b) B.H. Robinson, Chemistry and Reactivity of Metal Cluster Carbonyl Radical Anions in Paramagnetic Organometallic Species in Activation, Selectivity and Catalysis, Kluwer, Dordrecht, 1987;
(c) A.J. Bard, L.R. Faulkner, Electrochemical Methods, Wiley, New York, 1980;
(d) H. Yao, M. Sabat, R.N. Grimes, P. Zanello, F. Fabrizi de Biani, Organometallics 22 (2003) 2581;
(e) H. Yao, M. Sabat, R.N. Grimes, F. Fabrizi de Biani, P. Zanello, Angew. Chem. Int. Ed. Eng. 42 (2003) 1002;
(f) D. Osella, L. Milone, C. Nervi, M. Ravera, Eur. J. Inorg. Chem. (1998) 1473;
(g) A. Ceccon, S. Santi, L. Orian, A. Bisello, Coord. Chem. Rev. 248 (2004) 683.
[11] V.H. Nöth, L. Meinel, Z. Anorg. Allg. Chem. 349 (1967) 225.
[12] E.C. Lisic, B.E. Hanson, Inorg. Chem. 25 (1986) 812.
[13] J. Ellermann, N. Geheeb, G. Zoubek, G. Thiele, Z. Naturfosch. Teil B 32 (1977) 1271.
[14] C. Moreno, M.J. Macazaga, S. Delgado, Inorg. Chim. Acta 182 (1991) 55.
[15] D.R. Coulson, Inorg. Synth. 28 (1990) 107.
[16] Y.T. Park, I.K. Seo, Y.-R. Kim, Bull. Korean Chem. Soc. 17 (1996) 480.
[17] Z. Otwinowski, W. Minor, Methods Enzymol. 276 (1997) 307.
[18] G.M. Sheldrick, SHELXTL/PC V5.1, Bruker Analytical X-ray Systems, Madison, WI, USA, 1997.
[19] C. Moreno, M.J. Macazaga, R.M. Medina, D.H. Farrar, S. Delgado, Organometallics 17 (1998) 3733.
[20] (a) G. Váradi, A. Bici-Orisz, V. Sándor, G. Pályi, J. Organomet. Chem. 108 (1976) 225;
(b) L.S. Chia, W.R. Cullen, M. Franklin, A.R. Manning, Inorg. Chem. 14 (1975) 2521.
[21] R.K. Harris, Nuclear Magnetic Resonance Spectroscpy: A Physiochemical View, Pitman, London, 1983.
[22] (a) T.J. Snaith, P.J. Low, R. Rousseau, H. Pushmann, J.A.K. Howard, J. Chem. Soc., Dalton Trans. (2001) 292;
(b) E. Champel, S.M. Draper, J. Chem. Soc., Dalton Trans. (2001) 1440.
[23] A.L. Spek, PLATON, The University of Utrecht, The Netherlands, 2004.
[24] Average bite angle of dppm on Co–Co complexes determined to be 110.04° from analysis of Cambridge Crystallographic Database.
[25] C.E. Housecroft, B.F.G. Johnson, M.S. Khan, J. Lewis, P.R. Raithby, M.E. Robson, D.A. Wilkinson, J. Chem. Soc., Dalton Trans. (1992) 3171.
[26] G.J. Bezems, P.H. Rieger, S.J. Visco, J. Chem. Soc. Chem. Commun. (1981) 265.
[27] M. Arewgoda, P.H. Rieger, B.H. Robinson, J. Simpson, S.J. Visco, J. Am. Chem. Soc. 104 (1982) 5633.
[28] D. Osella, J. Fiedler, Organometallics 11 (1992) 3875.
[29] N. Duffy, J. McAdam, C. Nervi, D. Osella, M. Ravera, B.H. Robinson, J. Simpson, Inorg. Chim. Acta 247 (1996) 99.
[30] (a) M.L. Marcos, M.C. Moreno, A. Arnanz, S. Delgado, J. González Velasco, Port. Electrochim. Acta (in press);
(b) A. Arnanz, M.L. Marcos, C. Moreno, S. Delgado, J. González-Velasco, unpublished work.
[31] F. Diederich, Nature 369 (1994) 199.
[32] D. Osella, L. Milone, C. Nervi, M. Ravera, J. Organomet. Chem. 488 (1995) 1.
[33] (a) G.C. Allen, N.S. Hush, Prog. Inorg. Chem. 8 (1967) 357;
(b) M.B. Robin, D. Day, Adv. Inorg. Chem. Radiochem. 10 (1967) 247.
[34] R.P. Aggarwal, N.G. Connelly, M.C. Crespo, B.J. Dunne, P.M. Hopkins, A.G. Orpen, J. Chem. Soc., Dalton Trans. (1992) 655.
[35] C.J. McAdam, N.W. Duffy, B.H. Robinson, J. Simpson, Organometallics 15 (1996) 3935.
[36] J.A. McCleverty, M.D. Ward, Acc. Chem. Res. 31 (1998) 842.